LA-UR-96-2027

CONF-9606116--57

Title: Surface Roughness Measurements of Beta-Layered Solid Deuterium-Tritium in Toroidal Geometries

Author(s): J.K. Hoffer
L.R. Foreman
J.J. Sanchez
E. Mapoles
J.D. Sheliak

Submitted to: 12th Topical Meeting on the Technology of Fusion Energy
American Nuclear Society
June 16-20, 1996
Reno, Nevada
To appear in Fusion Technology

DISCLAIMER

SURFACE ROUGHNESS MEASUREMENTS OF BETA-LAYERED SOLID DEUTERIUM-TRITIUM IN TOROIDAL GEOMETRIES

James K. Hoffer & Larry R. Foreman
Los Alamos National Laboratory
Mail Stop K764
Los Alamos, New Mexico 87545
(505)667-4049/667-1846

Jorge J. Sanchez & Evan R. Mapoles
Lawrence Livermore National Laboratory
Mail Station L-482
Livermore, California 94551
(510)423-3553

John D. Sheliak
General Atomics, Inc
Mail Stop K764
Los Alamos, New Mexico 87545
(505)667-4077

ABSTRACT

New experiments in a NIF-scale toroidal cylinder have resulted in true shadowgraphs of the DT ice surface. The spectral analysis of the images summed over ℓ-modes 2 through 256 reveal that the surface roughness reaches values just below 1.0 μm at temperatures of 19 K and above. Summing only modes $\ell \geq 10$, the partial surface roughness is below 0.7 μm at 19.5 K. These results indicate that native beta-layering will be sufficient to meet the NIF requirements for DT ice surface finish for both Be and CH ablating shells.

The toroidal cylinder incorporates a linear heater along the cylindrical axis to test the concept of surface enhancement due to heat assisted beta-layering in DT. Additionally, with the use of this heater it is possible to symmetrize a pure D_2 layer.

I. INTRODUCTION

Inertial Confinement Fusion (ICF) experiments require highly uniform layers of liquid or solid deuterium-tritium (DT) fuel condensed on the inner surface of the target capsule. For the National Ignition Facility (NIF), the prototype ignition target has a plastic or beryllium shell approx. 150 μm-thick with an inside diameter of 1.5 mm surrounding a 80 μm-thick layer of DT.

Symmetric *liquid* layers of DT up to ~6 μm thick have been supported inside small glass microballoon targets using a thermal gradient technique[1]. Although thicker liquid layers have been supported[2] in NIF-scale capsules, they are unstable or highly non-uniform because the ratio of the surface tension force to the gravitational force becomes too small.

Highly uniform solid DT (or D_2) layers have been demonstrated using the "beta-layering" technique in both cylindrical[3] and spherical[4] geometries. However, the ice layer grown by beta-heating-driven sublimation-condensation is not amorphous and the surface finish attained by this natural process is a major concern for the application of this technique to ICF target fabrication. The inner surface of the fuel layer in laser fusion targets must be very smooth[5] to prevent implosively-driven Rayleigh-Taylor instabilities from mixing cold fuel into the hot spot.

Measurements of the surface roughness of a DT ice layer inside a transparent spherical target present difficulties because the layer is relatively thin and its inner edge lies close to the inner edge of the capsule wall. Furthermore, the image is distorted by the intervening ice and the refractive effect of the capsule itself. In a previous experiment using a re-entrant cylindrical cell to remove the refractive distortions associated with a spherical geometry, Sheliak[6] reported that the rms surface roughness, σ, for a 139 μm-thick DT ice layer was 1.7 μm. However, the surface measurements were affected by optical imperfections in the ice layers that formed on the sapphire windows used to seal the re-entrant cylinder.

In this paper we present results of new experiments designed to improve the accuracy and resolution of surface roughness measurements by removing many of the distortions which caused uncertainty in previous experiments. Additionally, with an integrated axial heater, we report the smoothing effect of a heat flux on the surface of hydrogen fuel layers formed on a *curved* substrate.

II. DESCRIPTION OF THE TOROIDAL TEST CELL

A cylindrical cell design with an internal toroidal geometry was used because it approximates the doubly curved geometry of a sphere (i.e., curvature in two orthogonal directions) while still permitting an unobstructed view of the hydrogen ice edge. The radius of the central bore at the waist is 1.00 mm and hence the cell has dimensions roughly equivalent to an NIF target. The design incorporates a central heater to provide the required heat flux for surface smoothing as depicted in Fig. 1.

The cell design was based on a thermal analysis finite element model[8] that incorporated the copper substrate, the axial heater, and the two glass windows. The goal of the thermal analysis was to insure that the shape of the isotherms near the surface of the copper torus would remain invariant upon the application of axial heater power. If

this were not done, the hydrogen ice layer would be subject to bulk migration due to a change in its thermal environment, causing the observed layer thickness to change noticeably whenever the heater power was changed. The thermal modeling led us to increase the poloidal radius to 1.50 mm and to truncate the torus as shown. By adjusting the thermal conductivity of the axial heater to lie in the range of 1.0 to 1.5 W/K, the portion of the of the heat shunted through the glass windows to the copper body of the torus could be controlled. This is advantageous because heat shunted through the glass windows helps keep them free of ice and secondly, the increased heat flux through the gas near the windows forces the isotherms to conform to the toroidal shape.

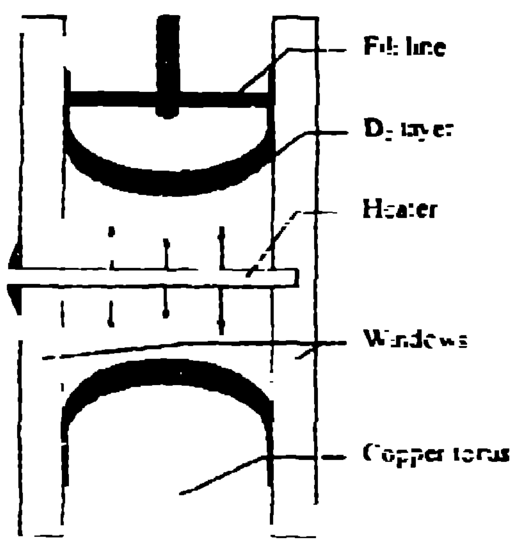

Fig. . Schematic cross-sectional view of the toroidal cell shown with a relatively thick equilibrated D_2 ice layer. Arrows represent heat emanating from the central heating rod. The clear bore is 2 mm in diameter while the poloidal radius is 1.5 mm.

The axial heater was constructed by winding two layers of #5[illegible] resistance wire onto a 125 μm-diameter mandrel and then epoxy potting the wound heater inside a [illegible] μm-OD gold tube to obtain the required thermal conductance. The heater assembly was inserted into the cell via a hole through one of the windows and sealed with epoxy. To avoid thermal stresses and possible leakage of tritium, the heater was not sealed into the far window but was accurately located in a small recess ground into it.

A narrow angle diffuse back light source similar in design to a Kohler microscope light was constructed to reduce the amount of light scattered into the ice layer. This back lighter produces images of the edge with a very high contrast ratio and excellent definition well suited for automated image analysis.

III. EXPERIMENT PROCEDURE

The toroidal cell was attached to the low temperature stage of a closed-cycle helium gas refrigerator located in a ventilated, tritium-approved hood[6]. It was connected to a gas handling system capable of providing either pure D_2 or DT. The cell was surrounded by a sealed secondary containment chamber kept evacuated to prevent ice crystals from condensing on the cell windows. Hence the thermal link to the cell was entirely due to its copper mounting stand. In use, the cell was cooled to just above the triple point of the gas mixture and a small amount of liquid hydrogen was condensed into it. Then the temperature of the cryostat was quickly lowered to the desired operating temperature between 12.0 K and 19.5 K.

To melt the ice layer between different experiments, the cell's temperature was brought slowly up to a few millikelvin above the triple point of the isotopic mixture and held at that temperature for a few minutes. Unfortunately melting was frequently accompanied by a gross change in the amount of hydrogen in the cell so that in practice it was not possible to make repeated experiments on layering at the same value of final layer thickness.

IV. DATA ACQUISITION AND REDUCTION

Each particular experiment consists of acquiring a series of high resolution CCD images of the developing ice layer[4]. Once the image data is acquired, it is transferred to a second computer where an image analysis program[4] determines the ice edge location along radial lines emanating from the center of the image versus angle and then performs an FFT to yield a modal perturbation power spectrum. The [illegible] of the ice layer is determined by taking the square root of the quadratically summed power spectrum over all modes of interest, typically modes 2 through 2[illegible]. Due to the large number of CCD pixels in the image (1024²), the high dynamic range of each pixel (12 bits) and the degree of integration inherent to the analysis, features as small as 0.1 μm rms are noticeable in the power spectrum[7]. Hence it was necessary to eliminate tiny particulates such as frozen methane by cleaning the incoming hydrogen with two separate 2 μm pore-size filters located at intermediate temperatures on the fill line [illegible] 15 μm filter located near the entrance to the cell.

V. D_2 EXPERIMENTS

Due to programmatic [illegible] few experiments were conducted with pure deuterium. Of [illegible] experiments using D_2 are [illegible] of the experimental cell [illegible]

ium. In addition, D_2 experiments permitted a calibration of the effective heat flux from the central heater.

Ignoring the effects of ^{3}He production (which can be quite significant, depending on sample age and temperature), a simple one-dimensional model[3] has proven to be sufficient to predict the rate constant r for the exponential approach to ice layer thickness uniformity inside spherical or cylindrical isothermal shells due to beta-layering in DT, giving

$$r = H_S / q, \qquad (1)$$

where H_S is the heat of sublimation (J/g) and q is the rate of heat generation (W/g) in solid DT. For DT at 19 K, r = 26.73 minutes, i.e., *independent of layer thickness*.

Using a one-dimensional argument similar to that used previously[3], we have derived the rate constant r_a appropriate for heat-assisted layering in D_2:

$$r_a = \frac{H_S \ \rho_s \ d}{Q \ (2\pi \cdot r_i)}, \qquad (2)$$

where ρ_s is the solid density, d is the final uniform layer thickness, Q is the lineal rate of heat production from the central heater (W/cm), and r_i is the internal ice radius. Note that $\frac{Q}{(2\pi \cdot r_i)}$ is equivalent to the heat flux at the inner ice surface (W/cm^2). Hence we predict that the redistribution rate constant due to a central heater (for relatively thin solid layers, where r_i is nearly constant) is *proportional to layer thickness* and inversely proportional to the heater power. The results of our preliminary D_2 experiments are consistent with these predictions, assuming that ~30 % of the heater power is shunted by the windows. Unfortunately, however, we did not allow sufficient time during the equilibration periods to accurately evaluate the rate constants as a function of heater power. (Currently, we are involved with further D_2 experiments to provide more accurate values.) Moreover, it is not strictly correct to assume that rate measurements made in the present "open" geometry are equivalent to those made in the "closed" geometry of a sphere or a straight cylinder. We can only observe layer evolution at one position in the torus, namely at the waist, but redistribution of material following a freeze from the melt can involve solid frozen on sections of the cell near the windows which are out of the field of view, resulting in slower rate observations.

We have been measuring the rate constant r_a by fitting an exponential to the σ values resulting from the data analyses. The final σ measured in the solid D_2 layer does not appear to be a strong function of heater power, saturating at ~1.9 μm at heater powers of 1 mW and above for an 80 μm-thick layer. However, our limited data does suggest that for D_2 ice, σ is roughly proportional to layer thickness.

VI. DT EXPERIMENTS

A. Native Beta-Layering

It proved to be very difficult to estimate the appropriate amount of liquid to condense into the cell in order to achieve the desired (NIF-target) solid thickness of 80 μm. The majority of the initial liquid charge is not visible as a meniscus and only after a lengthy layering equilibration is the final thickness of solid obvious. By luck, one of the experiments shown in Fig. 2 hit the desired 80-μm thickness exactly! Fig. 2 shows the evolution of three separate experiments where time is measured from the moment when the liquid DT charge is first frozen. The central heater was off for these experiments, thus only native beta-layering is driving the equilibration. We were not interested in rate measurements here but only the ultimate minimum in σ. In any case, it is not possible to evaluate σ at much earlier times, because it typically takes about one hour for the DT ice initially frozen on the windows to sublime away and permit a clear view of the interior toroidal surface.

The behavior shown in Fig. 2 is typical of all of our native beta-layering experiments in that σ minimizes five to six hours after first freezing. In our toroidal cell, some of the early time is spent redistributing the solid initially frozen on the windows. To the naked eye, the layer appears to be invariant after only two hours, but the effects seen here are subtle and can only be observed with the sensitive analysis discussed in section IV.

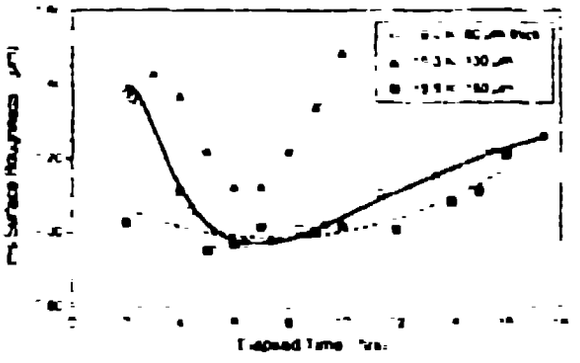

Fig. 2. RMS surface roughness vs. time for native beta-layering of DT.

The presence of a minimum σ in each data set is undoubtedly due to the production of ^{3}He in the solid layer. Our data on heat-assisted layering in pure D_2 show no such minima as long as the heater power is maintained constant. Typically, ^{3}He bubbles are observed "forming" within solid DT only at temperatures below ~18 K, although such details within the solid cannot be observed

with the present lighting system) Whether or not actual bubbles are present, it seems that sufficient ^{3}He forms within the solid to cause swelling or local distortions of the ice crystals. We can only conjecture that some DT crystallites, due either to their orientation or isotopic composition, swell at different rates from others. Whatever the cause, it is obvious that the degradation of the ice surface is sufficiently slow to allow for a considerable period of time during which a beta-layered target could be 'shot'. However, it is problematic that the minimum occurs so late, roughly ten rate constants, i.e., $\sim 10\cdot\tau$, after first freezing.

The good news is that the final σ is slightly below 1.0 μm for an 80 μm-thick layer at 19.0 K. The dramatic improvement in σ over previous data[6] in a re-entrant cylinder are due to improved optics, improved backlighting which gives a higher contrast of the interior ice edge, and most importantly, the presence of low thermal conductivity window material which allows the windows to become ice-free with only the very small self-heating present in the DT vapor space. We have estimated that the self heating in the vapor space of the prototype NIF target is approx. 1 μW at 19 K, due primarily to betas formed in the nearby solid depositing energy to molecules in the vapor space[16]. During our D_2 experiments we expressly used some very low heater powers to determine where the windows would just remain clear of ice. Factoring in the larger volume of the present torus over a spherical NIF target, the power necessary to remove D_2 ice is consistent with our estimations of beta-activated self-heating in DT vapor.

The data shown in Fig. 2 for a 130 μm thick layer at 19.0 K show both a higher minimum σ and a steeper rise after the minimum. The data prior to the minimum are also noticeably higher than the 80 μm-thick data. Both these observations are consistent with the additional DT solid thickness. At early times, relatively more material must be removed from the windows and the overall layering uniformity is delayed. At all times, the greater layer thickness produces a proportionally greater amount of ^{3}He. Hence the degrading effects of ^{3}He are increased and the net result is that the minimum σ occurs at roughly the same time as for the thinner layer. At a higher temperature of 19.5 K (only 0.3 K from the triple point) the data again minimize slightly below 1.0 μm at roughly six hours. Note that this layer is more than twice the thickness of the 80 μm-thick layer. The elevated temperature just makes up for the increased thickness, presumably because at elevated temperatures the ^{3}He can more easily diffuse out of the solid DT into the vapor space. This is consistent with the lower slope of increasing σ vs. time following the minimum seen in the data at 19.5 K, relative to that seen in the 130 μm thick layer at 19.0 K. We may only guess at how much smoother the 19.5 K data might have been if layer had not been so thick.

Figure 3 shows the ice layer surface roughness power spectrum a_l for the 80 μm-thick layer at 19.0 K at 324 minutes, which is near the minimum observed in Fig. 2.

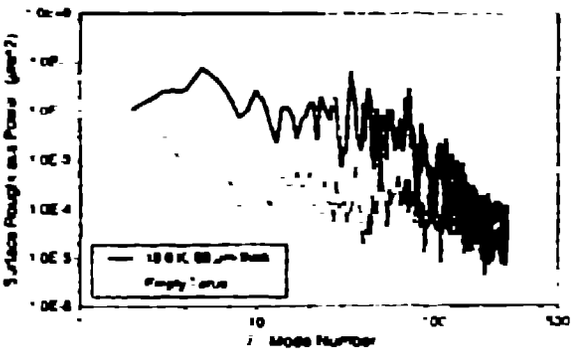

Fig. 3. Surface roughness power spectrum vs. l-mode number for native beta-layering of DT at 19 K.

Also shown is the power spectrum for the empty torus showing that an excellent job of machining was done on this difficult geometry[11]. Compared to the power spectra obtained in a re-entrant cylinder with sapphire windows[6], the present data are lower at all modes. Note that no single mode has an amplitude (obtained by taking the square root of any point on the power spectrum) above 0.1 μm.

Another method of displaying the spectral data is shown in Fig. 4, where we have plotted a partial surface roughness amplitude $\sigma_{p,}$ defined by

$$\sigma_{p,} = \sqrt{\sum_{l}^{256} a_l} \qquad (1)$$

This value computes the surface roughness summed for all modes at and above the value of l, e.g., the total σ is that shown at $l=2$ (the lowest mode which we can evaluate in the present experimental configuration) while $\sigma_{p,}$ is summed only for modes 10 and higher, etc. Such a plot allows one to evaluate the relative contribution of lower modes vs. higher modes to the total σ.

Comparing the native beta-layering $\sigma_{p,}$ obtained at 19.5 K with that measured at 19 K, we now see that at the higher temperature, there is less contribution to σ due to higher modes, while the contributions due to modes below $l = 10$ are higher, presumably due to the greater thickness of the layer. At higher temperatures, the layer is smoother because smoothness is primarily a manifestation of the amplitude of higher mode numbers, but the thicker layer is lumpier, i.e., it has greater low modal perturbations.

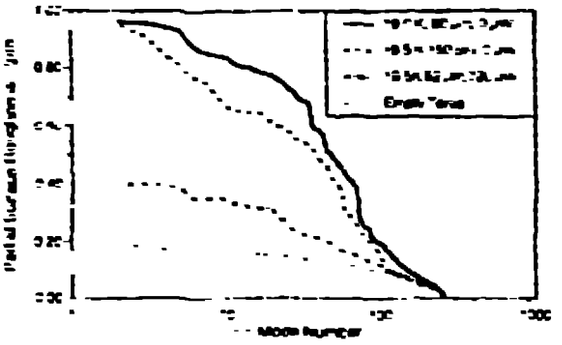

Fig. 4 Partial surface roughness σ_{pl} vs. mode number l for the empty cell, two native beta-layered DT surfaces, and a DT solid ice layer enhanced by an additional heat flux from an axial heater

B. Heat-Assisted Beta-Layering

Additionally, we present a spectrum in Fig. 4 measured for a relatively thin layer at 19.5 K, where a supplemental heater power of 720 μW was present during the layer formation. Some of the dramatic improvement in the overall σ_{rms} is undoubtedly due to the relative thinness of this layer. However, most of this improvement is due to the smoothing enhanced by the central heat flux. Note that there is relatively little contribution to the roughness due to modes above $l \approx 20$. This spectrum was that of the minimum in the time series, occurring only 30 min after freezing. Following the minimum, the layer did not degrade steadily as do native beta-layers, but ultimately leveled off at ~0.7 μm rms. A previous experiment was performed where the layer was first equilibrated with native beta-layering at 19.5 K, then after ~12 hours the heater was activated. In this case, σ_{rms} smoothly decreased to a final value again near ~0.7 μm within 150 minutes. We may hypothesize that a central heat flux can compensate for steady-state production of ^{3}He. However, for freshly frozen DT where ^{3}He has not yet saturated the solid, even smoother layers are possible for a brief period of time.

VIII. CONCLUSIONS

We should caution that our conclusions are rather tentative because we do not yet have a sufficient data base of other native beta-layering or heat-assisted DT beta-layering. More work on layering with DT will follow a thorough study of heat-assisted D$_2$ layering in the ionus now undergoing to identify and correct systematic errors.

Nonetheless, it appears that the technique of native beta-layering will be sufficient for providing sufficiently smooth ice layers for NIF ignition targets. Recent theoretical modeling[7] has shown that, for perfectly smooth plastic shell NIF targets and for perfect laser drive illumination symmetry, σ can be as great as 3 μm rms (8 μm rms when the shell material is beryllium). At only 1 μm rms, the DT ice surface roughness consumes only ~11 % (<2% for Be) of the total allowable roughness budget.[7]

REFERENCES

1. K. Kim, L. Mok, M. J. Erickborn, and T. P. Bernat, "Non-contact thermal gradient method for fabrication of uniform cryogenic inertial fusion target," *J. Vac. Sci. Technol.* A 3 (3), May/June 1985.

2. J. J. Sanchez et al., "Liquid Hydrogen Layers in Capsules of Large Diameter," Laser Interact. with Matter Conf., Oxford, 19-23 September 1994.

3. J. K. Hoffer and L. R. Foreman, "Radioactively Induced Sublimation of Solid Tritium," *Phys. Rev. Lett.* 60, 1310 (1988).

4. T. P. Bernat, E. R. Mapoles and J. J. Sanchez, "Temperature- and Age-Dependence of Redistribution Rates of Frozen Deuterium-Tritium," Inertial Confinement Fusion Quarterly Report 1(2), Lawrence Livermore National Laboratory, Livermore, CA, UCRL-LR-105821-91-2, pp. 57-61, (1991). John D. Simpson, James K. Hoffer and Larry R. Foreman, "Beta Layering of Solid Deuterium-Tritium in a Spherical Polycarbonate Shell," *Fusion Technology*, 21, 330, (1992).

5. S. Yuan, S. Pellone, J. Lindl, et al., ICF Quarterly Report 5(2), Lawrence Livermore National Laboratory, Livermore, CA, UCRL-LR-105821-95-4, p. 81, (1995).

6. J. D. Sheliak, J. K. Hoffer, L. R. Foreman, and E. R. Mapoles, "High Resolution Optical Measurements of Solid Surface Roughness for Beta-Layered D-T Inside a Re-entrant Copper Cylinder," (to be published in *Fusion Technology*, September, 1996).

7. G. Collins, E. Mapoles, et al., Solid Hydrogen Surfaces," Inertial Confinement Fusion Quarterly Report 3 (2), Lawrence Livermore National Laboratory, Livermore, CA, UCRL-LR-105821-93-2, pp. 81-89, (1993).

8. "COSMOS," Structural Research and Analysis Corporation, 12121 Wilshire Blvd., Los Angeles, CA 90025-1172, ph: (310) 207-2800.

9. E. R. Mapoles, E. Hinkel, and R. Wallace, "Measurements of the Sensitivity Limits of Shadowography," Technical Note TA1 95-052, June 29, 1995, Lawrence Livermore National Laboratory, Livermore, CA.

10. P. C. Souers, *Hydrogen Properties for Fusion Energy*, University of California Press, Berkeley, California, (1986).

11. The toroidal cell was machined by Art Demuth and assembled by Jim Pipes (both at LLNL).

12. William J. Krauser, et al., "Ignition Target Design and Robustness Studies for the National Ignition Facility," Phys. Plasmas, 3 (5), pp. [illegible].